Journal of Luminescence 169 (2016) 43–50

Contents lists available at ScienceDirect

Journal of Luminescence

journal homepage: www.elsevier.com/locate/jlumin

# Optical and scintillation properties of $Ce^{3+}$-doped $YGd_2Al_{5-x}Ga_xO_{12}$ ($x=2,3,4$) single crystal scintillators

Warut Chewpraditkul [a], Petr Brůža [b], Dalibor Pánek [b], Nakarin Pattanaboonmee [a], Kriangkrai Wantong [a], Weerapong Chewpraditkul [a,*], Vladimir Babin [c], Karol Bartosiewicz [c], Kei Kamada [d], Akira Yoshikawa [d], Martin Nikl [c]

[a] Department of Physics, King Mongkut's University of Technology Thonburi, Bangkok 10140, Thailand
[b] Faculty of Biomedical Engineering, Czech Technical University in Prague, Kladno, Czech Republic
[c] Institute of Physics, AS CR, Cukrovarnicka 10, Prague 16253, Czech Republic
[d] IMR, Tohoku University, 2-1-1 Katahira, Aoba-ku, Sendai 980-8577, Japan

ARTICLE INFO

*Article history:*
Received 16 January 2015
Received in revised form
31 August 2015
Accepted 1 September 2015
Available online 8 September 2015

*Keywords:*
$YGd_2Al_{5-x}Ga_xO_{12}$:Ce
$Y_3Al_5O_{12}$:Ce
Light yield
Luminescence
Scintillation

ABSTRACT

The optical and scintillation properties of $Ce^{3+}$-doped $YGd_2Al_{5-x}Ga_xO_{12}$ ($x=2,3,4$) single crystals were investigated. With increasing Ga content in the garnet host, the $5d_1$ absorption and emission bands shift toward higher energy due to the decrease in the crystal field splitting of the 5d levels. Temperature dependences of absorption and emission spectra and of photoluminescence decays of both prompt and delayed components were measured. Light yield (LY) and its dependence on an amplifier shaping time were measured under excitation with γ-rays. High LY value of 38,000 photons/MeV was obtained for a $YGd_2Al_2Ga_3O_{12}$:Ce sample. Scintillation decay was measured with an extended dynamical and temporal scale under the nanosecond-pulsed soft X-ray excitation. The relative content of the fastest component in the scintillation response increases with increasing Ga content.



## 1. Introduction

$Ce^{3+}$-doped $Y_3Al_5O_{12}$ (YAG:Ce) and $Lu_3Al_5O_{12}$ (LuAG:Ce) single crystals are prospective scintillator materials due to their high light yield (LY) and fast decay time [1–4]. However, their scintillation performance is strongly degraded by the presence of shallow electron traps which delay an energy transfer to the $Ce^{3+}$ emission centers and give rise to intense slow components in the scintillation decay [5,6]. Consequently, the measured LY values for LuAG:Ce are about 14,000–25,000 photons/MeV [7,8] while the theoretical LY limit for the aluminum garnet scintillators was estimated to be about 60,000 photons/MeV [9]. Partial substitution of $Al^{3+}$ with $Ga^{3+}$ in the aluminum garnet diminishes the trapping effects of shallow electron traps [10] but the bottom of the conduction band decreases [11] and gets closer to the 5d level of $Ce^{3+}$ center at the same time. This leads to unwanted thermal ionization of the lowest 5d level ($5d_1$) of the $Ce^{3+}$ emission center which reduces the scintillation efficiency [12]. However, it is possible to lower the position of $5d_1$ level which increases the ionization energy by an admixture of larger Gd cations into the aluminum garnet host. Therefore, $Ce^{3+}$-doped $(Gd, RE)_3(Ga, Al)_5O_{12}$, RE=Lu, Y multicomponent garnets were intensively investigated [13–15] and provided high LY values up to 50,000 photons/MeV. The fundamental aspects of the energy transfer processes in the multicomponent garnet and interaction of trivalent rare earth ($RE^{3+}$) emission centers with the host became of broad interest [16–19]. Development of this family of fast, efficient and high density garnet scintillators within the last decade has been recently reviewed [20].

In this work, the optical and scintillation characteristics of the $Ce^{3+}$-doped $YGd_2Al_{5-x}Ga_xO_{12}$ ($x=2,3,4$) single crystals were investigated. We characterize the change in the crystal field splitting and the transition energies of 5d levels by absorption, photoluminescence excitation (PLE), and emission (PL) spectra measurements. Specifically, temperature dependence of prompt and delayed PL decay components was measured to reveal thermally induced ionization processes in the $5d_1$ excited state of $Ce^{3+}$ center. The LY and its dependence on the amplifier shaping time were also measured in order to investigate the influence of Ga content on timing characteristics of scintillation response for the studied crystals. Finally, scintillation decay was measured in an extended dynamical and temporal scale under excitation with nanosecond-pulsed soft X-rays (SXR).

* Corresponding author. Tel.: +66 24708944.
*E-mail address:* weerapong.che@kmutt.ac.th (W. Chewpraditkul).

http://dx.doi.org/10.1016/j.jlumin.2015.09.001
0022-2313/

## 2. Experimental

$YGd_2Al_{5-x}Ga_xO_{12}$:Ce1% ($x$=2,3,4) single crystal samples were cut from the parent crystal rods prepared by a micro-pulling down method [15]. Polished plates of ∅3 mm × 0.5 mm were prepared and used for all measurements. Polished plate of 7 × 7 × 1 $mm^3$ commercial YAG:Ce single crystal grown by the Czochralski method in CRYTUR, Czech Republic, was used as a reference sample.

The PL and PLE spectra in the UV/Visible region were measured with a Hitachi F-2500 fluorescence spectrophotometer. Absorption spectra in the UV/Visible region were recorded by the Perkin Elmer Lambda 35, UV–vis spectrophotometer. LY measurements were performed under the 662 keV γ-ray excitation using a photomultiplier (PMT) based-setup described in [21]: the signal from a Photonis XP5200B PMT anode was sent to a CANBERRA 2005 preamplifier and then to a Tennelec TC243 spectroscopy amplifier. The PC-based multichannel analyzer (Tukan 8 k MCA) was used to record the pulse-height spectra. Gaussian function was fit to the full-energy peaks by using procedures in the MCA to determine their positions. The photoelectron yield, expressed as a number of photoelectrons per MeV (phe/MeV) of γ-ray energy deposited in the crystal, was determined by means of a single photoelectron method [21,22]. In this method the number of photoelectrons is measured by comparing the position of a full-energy peak of 662 keV γ-rays with that of the single photoelectron peak in pulse-height spectra. To improve the light collection efficiency the samples were coupled to the PMT window with silicone grease and covered with several layers of teflon tape.

The temperature dependences of PL decay curves were measured in the prompt decay (measured over the 1000 ns time window) and delayed recombination decay (measured over the 40 ms time window) using the custom made 5000 M spectrofluorometer (Horiba Jobin Yvon) equipped with TBX-04 photon counting detector (IBH, UK), for details see Ref. [23]. In the former experiment a nanosecond-pulsed LED was used as an excitation source for the decay measurements using the time-correlated single photon counting technique. In the latter one a microsecond-pulsed xenon flashlamp was used as an excitation source for the delayed recombination decay measurements using a standard multichannel scaling method. Given the high intensity of luminescence signals and low noise of our photon counting detector, the errors of reported quantities in photoluminescence characteristics are certainly below 1%.

The scintillation decay was measured under the excitation by nanosecond-pulsed SXR photons from the infrared laser-produced plasma in gaseous argon target. The 400 nm Ti foil was used as a soft X-ray band-pass filter. The sample was then excited by an incoherent SXR photon burst with the FWHM duration of 4.7 ns (Ref. [24]) and photon energy in the spectral range of 350–450 eV [25] for which the attenuation length of the SXR photons is of a few hundreds nanometers. In the detection part a quartz collection lens, Thorlabs FB550–40 (550 nm/40 nm FWHM) dielectric band-pass filter, and a Hamamatsu R7056 fast PMT operated in the direct current mode were used to detect scintillation light. The instrumental response function (IRF) was obtained by measurement of spectrally unresolved scintillation decay of superfast Ga-doped ZnO powder (scintillation response below 1 ns) under the same experimental conditions.

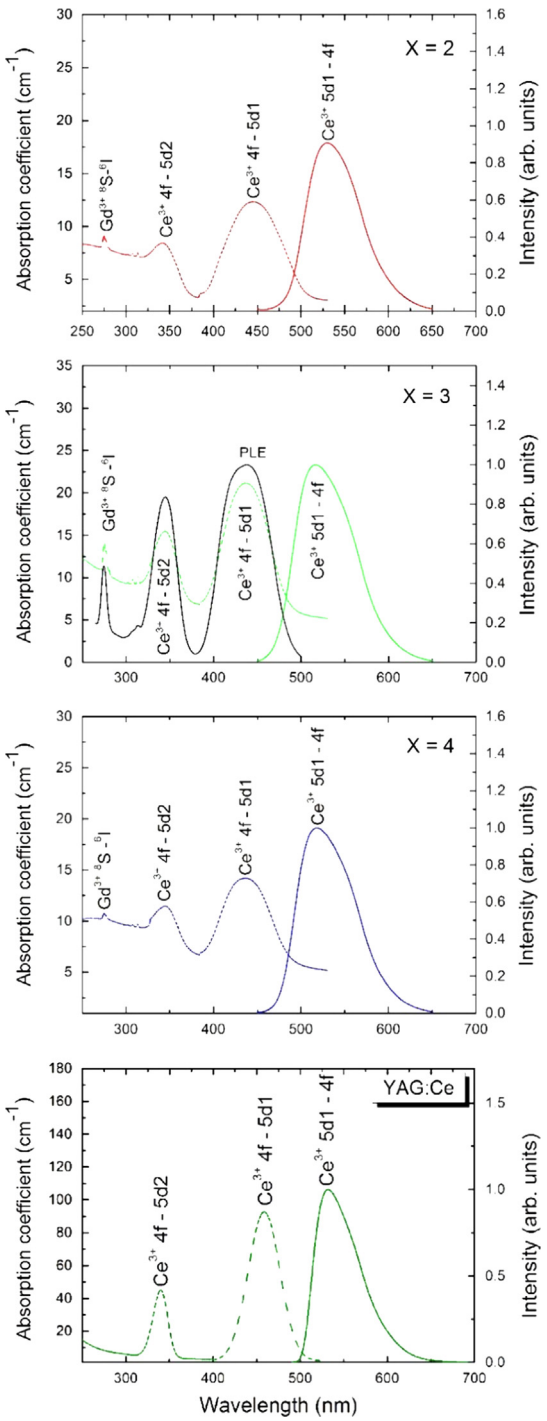


**Fig. 1.** Absorption (dashed line), PL and PLE (solid line; $\lambda_{em}$=510 nm was set for $x$=3) spectra of the $YGd_2Al_{5-x}Ga_xO_{12}$:Ce and YAG:Ce.

## 3. Results and discussion

### 3.1. Absorption and photoluminescence spectral characteristics

The absorption spectra, the PL spectra excited at 430 nm, and the PLE spectra (for $x$=3 only) of the $Ce^{3+}$ emission from the $YGd_2Al_{5-x}Ga_xO_{12}$:Ce and YAG:Ce samples are shown in Fig. 1. In the absorption spectra, two dominant bands are related to the 4f→5$d_1$ (between 385 and 500 nm) and 4f→5$d_2$ (between 325 and 370 nm) transitions of the $Ce^{3+}$, respectively. Weak line at 274 nm observed in both the absorption and PLE (see example for $x$=3 in Fig. 1) spectra is due to $^8S_{7/2}$ → $^6I_J$ transitions of $Gd^{3+}$ ions. Its presence in the excitation spectra indicates that the $Gd^{3+}$ → $Ce^{3+}$ energy transfer takes place in the $YGd_2Al_{5-x}Ga_xO_{12}$:Ce crystals as reported in more detail in Ref. [26]. Such energy transfer is enabled by the partial overlap of the $Gd^{3+}$ emission line at 314 nm (starting from $^6P_{7/2}$ level) [27] with the high energy side of 4f→5$d_2$ absorption band of

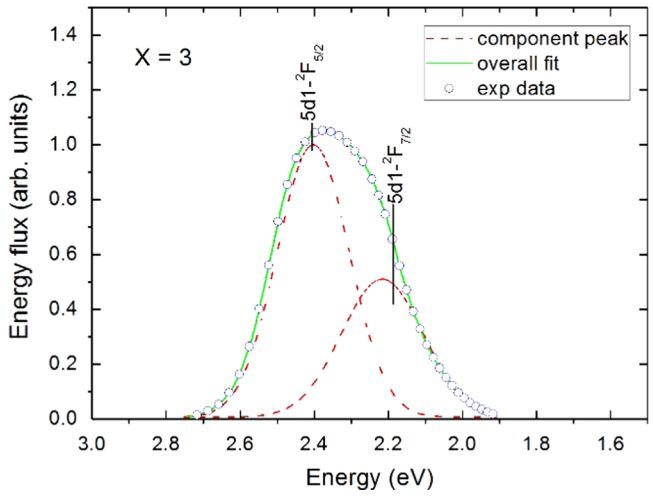


**Fig. 2.** Decomposition of $YGd_2Al_2Ga_3O_{12}$:Ce emission spectrum into two Gaussian components.

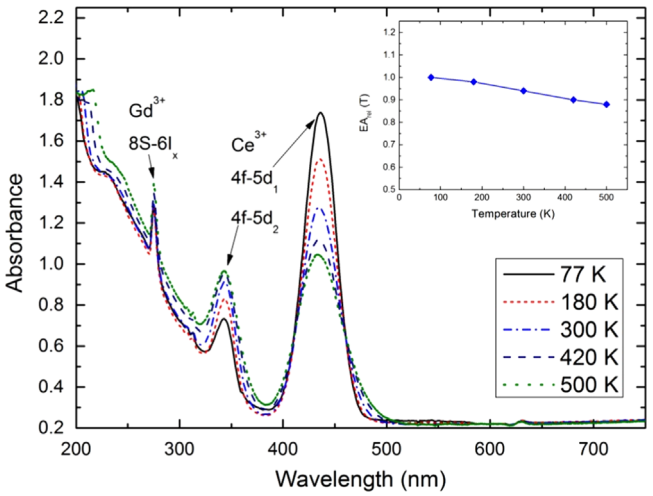


**Fig. 3.** Temperature dependence of absorption spectra of $YGd_2AlGa_4O_{12}$:Ce. The inset shows the relative decrease of absorbed excitation energy at 435 nm at increasing temperature compared to 77 K.

**Table 1**
The $Ce^{3+}$ absorption and emission transition energies in $YGd_2Al_{5-x}Ga_xO_{12}$:Ce at RT. The errors of the values derived from absorption spectra are typically below 1 nm, in the emission/excitation spectra ± 2 nm and in the Gaussian decomposition it is up to ± 3% due to larger overlap of Gaussian curves, see Fig. 2.

| Sample | Absorption | | | Emission | Stokes shift (eV) |
|---|---|---|---|---|---|
| | $4f–5d_1$ band (eV) | $4f–5d_2$ band (eV) | Splitting (eV) | $5d_1–{}^2F_{5/2}$ band (eV) | |
| YAG:Ce ref | 2.70 (459 nm) | 3.66 (339 nm) | 0.96 | 2.33 (532 nm) | 0.37 |
| $YGd_2Al_3Ga_2O_{12}$:Ce | 2.76 (449 nm) | 3.60 (344 nm) | 0.84 | 2.35 (528 nm) | 0.41 |
| $YGd_2Al_2Ga_3O_{12}$:Ce | 2.80 (442 nm) | 3.59 (345 nm) | 0.79 | 2.38 (521 nm) | 0.42 |
| $YGd_2AlGa_4O_{12}$:Ce | 2.83 (438 nm) | 3.57 (347 nm) | 0.74 | 2.41 (514 nm) | 0.42 |

$Ce^{3+}$ center. Luminescence bands due to the $Ce^{3+}$ $5d_1 \rightarrow 4f$ transitions were observed in all samples in the range between 460 and 600 nm. Double peak shape of the PL spectra consists of two $5d_1 \rightarrow {}^2F_{5/2}$ and $5d_1 \rightarrow {}^2F_{7/2}$ transitions and the transition energies were determined using two Gaussian-function fits to the PL spectrum plotted on an energy scale (see example in Fig. 2). Although the $4f \rightarrow 5d_2$ absorption peak shifts to lower energy with the increasing Ga content, the $4f \rightarrow 5d_1$ one shifts to higher energy and the $5d_1 \rightarrow 4f$ emission peak as well. Such a dependence on $Ga^{3+}$ content well corresponds to general trends summarized in [16,17–19,28,29]. Table 1 presents transition energies of the absorption and $5d_1 \rightarrow {}^2F_{5/2}$ emission peaks of $Ce^{3+}$ in the studied samples extracted from Fig. 1. The energy difference (splitting) between the $5d_1$ and $5d_2$ levels is provided for all samples.

The decrease in the splitting energy indicates that the crystal field strength around $Ce^{3+}$ at the dodecahedral site is reduced with increasing $Ga^{3+}$ content at the tetrahedral site [17–19,30]. The Stokes shift of about 0.42 eV in $Ce^{3+}$ center for the $YGd_2Al_{5-x}Ga_xO_{12}$:Ce samples is larger than that of about 0.37 eV for YAG:Ce. The decrease of both the crystal field strength and the band gap with increasing $Ga^{3+}$ content was found by means of electronic band structure calculations from the first principles in $Y_3Ga_xAl_{5-x}O_{12}$:Ce ($x$=0–5) [31] and from correlated DFT calculations and several optical experiments in Ce- and Eu-doped $Lu_3Ga_xAl_{5-x}O_{12}$ [11]. It results in the decrease of an ionization energy accompanied by the luminescence quenching due to thermal ionization of the $5d_1$ level of $Ce^{3+}$ emission center [17–19]. This phenomenon suggests us to investigate the influence of Ga content on the PL decay kinetics and scintillation characteristics for the $YGd_2Al_{5-x}Ga_xO_{12}$:Ce crystals which is further completed by temperature dependence of absorption spectra (Fig. 3) and PL spectra integral (Fig. 4) for selected samples.

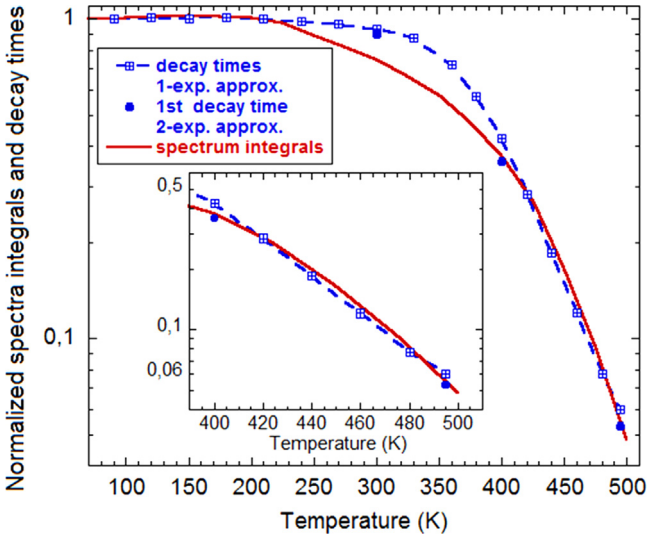


**Fig. 4.** Temperature dependence of normalized emission spectrum integral ($\lambda_{ex}$=435 nm) and decay time values obtained from one exponential and two-exponential (only selected temperatures from Fig. 5, shorter decay time value displayed only) approximations in $YGd_2AlGa_4O_{12}$:Ce. In the inset temperature region 400–500 K is displayed in detail. The emission spectrum integrals values are corrected for temperature dependence of the deposited excitation energy (from Fig. 3 inset).

In the absorption spectra in Fig. 3 clear interchange of absorption amplitudes is obtained between $4f \rightarrow 5d_1$ and $4f \rightarrow 5d_2$ bands of $Ce^{3+}$ which is analogous to the characteristics of $Ce^{3+}$ center in YAG host [32] and is due to different transition dipole moment from two lowest sub-levels in the ${}^2F_{5/2}$ ground state multiplet towards $5d_1$ and $5d_2$ excited states of $Ce^{3+}$. Considering the attenuation of optical beam intensity in the absorption measurement as

$$I(T) = I_0 \times 10^{-OD(T)} \quad (1)$$

where $I(T)$ is the intensity of outgoing light at temperature $T$, $I_0$ is

the intensity of incident light and OD($T$) is the optical absorbance at temperature $T$ (reflection losses subtracted), we get the intensity of outgoing light at temperature $T$. The ratio $I(T)/I_0$ is the fraction of incident light intensity transmitted through the sample, and $[I_0-I(T)]/I_0=1-10^{-OD(T)}$ is the fraction of incident light intensity absorbed in the sample. We can define the fraction of absorbed light energy at the lowest temperature 77 K: $1-10^{-OD(77\ K)}$ as 100%, then the relative decrease of the absorbed energy $EA_{rel}$ ($T$) in the sample at given temperature $T$ can be calculated by the following relation:

$$EA_{rel}(T) = [I_0 - I(T)]/[I_0 - I(77\ K)] = \left[1 - 10^{-OD(T)}\right]/\left[1 - 10^{-OD(77\ K)}\right]. \quad (2)$$

The decrease of $EA_{rel}$ ($T$) with increasing temperature is shown in the inset of Fig. 3. This dependence can be directly used to correct further the temperature dependence of emission spectrum integral measured in an independent experiment (Fig. 4). Temperature dependence of emission spectrum integral under excitation at 435 nm (max. of $4f\rightarrow 5d_1$ absorption transition of $Ce^{3+}$) is displayed in Fig. 4 for the $x=4$ sample including correction for the decreasing excitation energy deposited in the sample (inset of Fig. 3).

### 3.2. Photoluminescence decay kinetics characteristics

To reveal processes acting in the excited state of $Ce^{3+}$ emission centers and distinguish between thermal quenching and relaxed excited state ionization, the temperature dependence of prompt and delayed radiative recombination processes was monitored. This was done by measurement of prompt and delayed recombination decays in submicrosecond and millisecond time ranges, respectively. In Fig. 5 examples of prompt PL decays are shown at 180, 300, 400 and 500 K for the same sample $x=4$ as in Fig. 4 and single and double exponential approximations are shown by lines to calculate the decay time values. While the single exponential fit is an excellent approximation below 100 K, a slower tail and noticeable deviation from single exponential profile is observed at all temperatures above approx. 150 K. Such result points to the presence of the delayed radiative recombination process most probably due to ionization of the relaxed $5d_1$ excited state of $Ce^{3+}$ emission centers which is supported by the data in Fig. 7 below.

In Fig. 6 we present the temperature dependence of nanosecond decay times evaluated from the single exponential approximations of the prompt decay component for all three $YGd_2Al_{5-x}Ga_xO_{12}$:Ce ($x=2,3,4$) samples studied to show qualitative influence of gallium content. Similarly to what was seen in other compositions of multicomponent garnets [17,18,33] the onset of the decay time shortening occurs at lower temperature $T_0$ as the gallium content increases. Defining $T_0$ at 90% of the radiative lifetime value (decay time value at the lowest temperature, $T=8$ K, $Ce^{3+}$ luminescence quantum yield of 100%) we obtain $T_0=380$, 337 and 325 K for $x=2$, 3 and 4, respectively. It is interesting to note rather different values of temperatures $T_0$ in a similar sample set $Y_2GdAl_{5-x}Ga_xO_{12}$:Ce ($x=2,3,4$) with lower Gd content recently published [33]. In the latter sample set these values are estimated as $T_0=425$, 408 and 240 K for $x=2$, 3 and 4, respectively. The difference can be understood as a result of an interplay between the effects of $Gd^{3+}$ (increasing the ionization barrier and decreasing that of thermal quenching) and those of $Ga^{3+}$ (decreasing the ionization barrier and increasing that of thermal quenching) cations on the $5d_1$ excited state of $Ce^{3+}$ and bottom of the conduction band which gets decreased by both of them [12,17,18,34,35]. We have calculated the energy barrier governing the decay time decrease with temperature following a single barrier model.

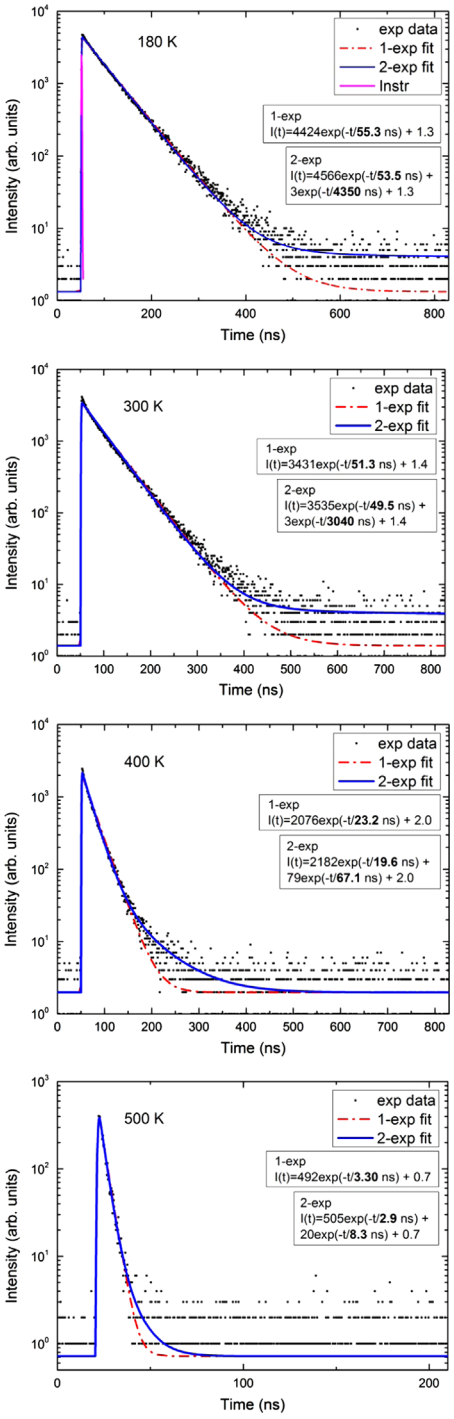


**Fig. 5.** Examples of PL decays of $YGd_2AlGa_4O_{12}$:Ce sample ($\lambda_{ex}=452$ nm, $\lambda_{em}=520$ nm).at 180, 300, 400 and 500 K and their single (dashed line) and double (solid line) exponential approximations. The lines (fit) are convolutions of instrumental response (instr, shown for 180 K only) and function $I(t)$ in each figure.

$$1/\tau(T) = 1/\tau_0 + W \times \exp(-E_a/kT) \quad (3)$$

where $\tau(T)$ is the decay time at $T$ ($K$), $\tau_0$ is the radiative lifetime value (at 8 K), W is the frequency factor, $E_a$ is the energy barrier for the quenching process, and $k$ is the Boltzmann constant. The obtained values of $E_a$ and $W$ for the studied samples are shown in the inset of Fig. 6. From $E_a$ values it follows that energy barrier decreases with increasing $Ga^{3+}$ content. Given the shape of PL decay at temperatures above RT, see examples in Fig. 5, the participation of thermal ionization of the $5d_1$ excited state of $Ce^{3+}$

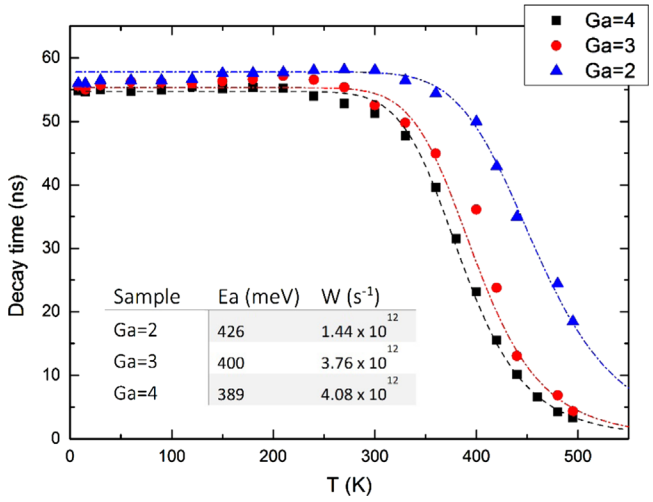


**Fig. 6.** Temperature dependence of the PL decay times of prompt decay component in the $YGd_2Al_{5-x}Ga_xO_{12}$:Ce ($x$=2,3,4) sample set. Dashed lines come from the Eq. [3] model described in the text.

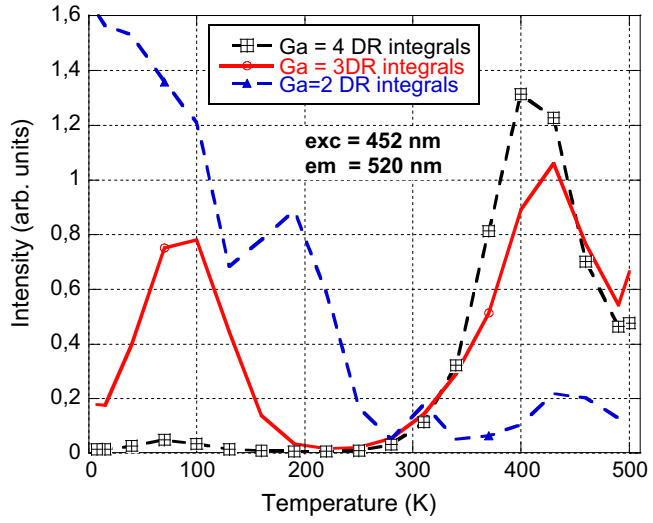


**Fig. 7.** Temperature dependence of integrals of the delayed recombination decay at $YGd_2Al_{5-x}Ga_xO_{12}$:Ce ($x$=2,3,4) sample set measured over 0–40 ms time window.

emission centers towards the conduction band can explain the appearance of slower tails in the decay. Comparing temperature dependence of normalized PL emission spectra integrals and decay time values in Fig. 4, it is worth noting the following: (i) Within 200–400 K the absolute decrease of emission spectrum integral intensity is somewhat bigger compared to the decay time decrease. There is no explanation at hand for such an effect and it needs further investigation; (ii) Comparing the values between 400 and 500 K, where the major intensity and decay time decrease occur, both dependences are closely similar. Consequently, within 400–500 K, thermal quenching process is the dominant one, and thermally induced ionization of the $Ce^{3+}$ $5d_1$ excited state provides rather negligible contribution to temperature dependence of the prompt decay process.

In Fig. 7 the temperature dependence of delayed recombination decay integrals is displayed (for technical details, see Refs. [23,33]). With increasing gallium content the effect of thermally-induced ionization of $5d_1$ excited state becomes evident above approx. 250–300 K which is enabled by higher sensitivity of this technique compared to the evaluation inferred from temperature dependences of emission spectrum integrals and nanosecond decay times in Fig. 4 above. The profile of the signal at higher temperatures can be further shaped by characteristics of traps participating in the delayed recombination (see the model in Ref. [36]). Complex thermoluminescence glow curves consisting of at least three peaks with evaluated trap depths within 0.88–1.14 eV were observed in this kind of multicomponent garnets [37]. However, in contrast to the situation in the $Y_2GdAl_{5-x}Ga_xO_{12}$:Ce ($x$=2,3,4) sample set reported in [33] the onset temperature of a ionization process practically does not change for $x$=3 and 4. This observation can be explained by the beneficial effect of increased Gd concentration which counteracts in the decrease of ionization barrier. It is also worth noting rather different course of the curves in Fig. 7 below RT; an intense signal even increasing towards low temperature can be due to involvement of shallow traps into the delayed recombination mechanism [36] or direct interaction with nearby defect energy levels in the forbidden gap. We also note that recent thermally stimulated luminescence study at $Gd_3Ga_3Al_2O_{12}$:Ce multicomponent garnet proposed the existence of wide quasi-continuous distributions of trapping levels to explain broad glow curve peak below 140 K [38]. The existence of broad trap-depth distribution might be enabled by atomistic fluctuation of composition in solid solutions which was proposed in several material groups as a reason for scintillation LY increase compared to limit compositions [39].

In the attempt to further resolve the contribution from the thermally induced (into conduction band) and a subgap delayed recombination processes at the lowest temperatures we can recall the key equation describing the temperature dependence of the delayed recombination emission intensity in the former case, coming from the model in Ref. [36]

$$I(T) = \text{const} \times e^{-\frac{E_a}{kT}} \sum_{i=1}^{n} A_i \left(e^{-\frac{t_1}{\tau i(T)}} - e^{-\frac{t_2}{\tau i(T)}}\right) \quad (4)$$

where the exponential term with $E_a/kT$ is a fraction of charge carriers thermally ionized ($E_a$ is an activation energy of thermal ionization) and the sum determines a number of charge carriers that get trapped and released from traps with the detrapping time falling into the time window of the measurement (for details see [36]). The most striking situation is found in $x$=2 sample when we compare the signal intensity in Fig. 7 at RT and 8 K: it is about 20 times higher at 8 K. However, at the same time the number of thermally ionized charge carriers in (4) is essentially zero while it significantly increases at RT. Consequently, the intensity due to thermal ionization $I$ (8 K) in (4) is also zero. Therefore, one cannot observe the course of delayed recombination intensity as in Fig. 7 ($x$=2), namely the high intensity signal at lowest temperatures, unless there is also some subgap process at work the origin of which is unclear, however, and needs further investigation. We also note that we have checked the emission spectrum of the delayed recombination process at $T$=8 K using microsecond flash lamp excitation and the reconstruction of emission spectrum from the decay curves integration in the time window 0.16–40 ms (see Ref. 40 for technical details) made with the step of 6 nm within 470–670 nm spectral region under excitation at the maximum of $4f \rightarrow 5d_1$ absorption band at 435 nm for the sample showing the most intense signal towards low temperatures ($x$=2). The spectrum perfectly coincides with the steady-state one which proves that the delayed recombination signal indeed comes from the $Ce^{3+}$ centers.

### 3.3. Scintillation characteristics

The pulse-height spectra under excitation by γ-rays from a $^{137}Cs$ source measured at 4 μs shaping time for these $YGd_2Al_{5-x}Ga_xO_{12}$:Ce and YAG:Ce samples have been recently reported in [41]. The obtained LY values are summarized in Table 2. Interestingly,

**Table 2**
Light yield, ratio of LY(0.5 μs) to LY(12 μs) and $K_{f/e}$ values for $YGd_2Al_{5-x}Ga_xO_{12}$:Ce crystals.

| Crystal | LY (Ph/MeV) | LY(0.5 μs)/LY(12 μs) (%) | $K_{f/e}$ (%) |
|---|---|---|---|
| $YGd_2Al_3Ga_2O_{12}$:Ce | 21,400 ± 2100 | 42 | 27 |
| $YGd_2Al_2Ga_3O_{12}$:Ce | 38,000 ± 3800 | 62 | 55 |
| $YGd_2AlGa_4O_{12}$:Ce | 35,600 ± 3600 | 71 | 66 |
| YAG:Ce | 27,700 ± 2800 | | |

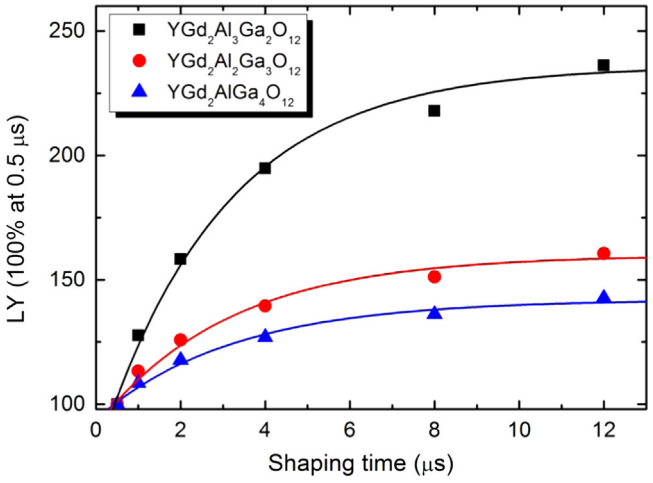


**Fig. 8.** Dependence of relative LY on amplifier shaping time normalized at 0.5 μs for $YGd_2Al_{5-x}Ga_xO_{12}$:Ce crystals. Solid lines come from the model described in the text.

$YGd_2Al_3Ga_2O_{12}$:Ce with all $Al^{3+}$ at octahedral sites occupied by $Ga^{3+}$exhibits lowest LY value but as soon as the $Ga^{3+}$ ion starts substituting into tetrahedral sites in $YGd_2Al_2Ga_3O_{12}$:Ce the LY value increases. This result can be attributed to the decrease of the band gap and the diminished trapping effect of shallow electron traps introduced by the Ga-admixture into the aluminum garnet host [10,11] which leads to dramatic LY increase. The measured LY value for $YGd_2Al_2Ga_3O_{12}$:Ce is about 37% higher than that of a reference YAG:Ce crystal. Somewhat decreasing LY value obtained for $YGd_2AlGa_4O_{12}$:Ce can be attributed to further decrease in the band gap and in the crystal field splitting, which reduces the energy difference between the $5d_1$ excited state and the bottom of the conduction band. It leads to luminescence quenching due to thermal ionization of $5d_1$ excited state of $Ce^{3+}$ emission center [17–19].

In order to investigate the acceleration in the scintillation response of $YGd_2Al_{5-x}Ga_xO_{12}$:Ce, the LY dependence on amplifier shaping time was measured under γ-ray excitation. As clearly seen in Fig. 8, there is very high contribution of slow scintillation light for $YGd_2Al_3Ga_2O_{12}$:Ce, indicating to much higher content of shallow electron traps which delay the energy transfer to $Ce^{3+}$emission centers and leads to a decrease of LY value. It demonstrates a remarkable decrease of slow component content in the scintillation response of $YGd_2Al_{5-x}Ga_xO_{12}$:Ce with increasing $Ga^{3+}$ content, resulting to an enormous increase of LY value. This result can be attributed to the diminished trapping effect of shallow electron traps [10] which fall into the bottom of the conduction band [11] and consequently the energy transfer from host to the $Ce^{3+}$ emission centers significantly accelerated.

Based on a two-exponential approximation of scintillation decay the normalized LY($t$) time dependence can be fitted by function

$$LY(t) = m_1 - m_2 exp(-m_3 t), \quad (5)$$

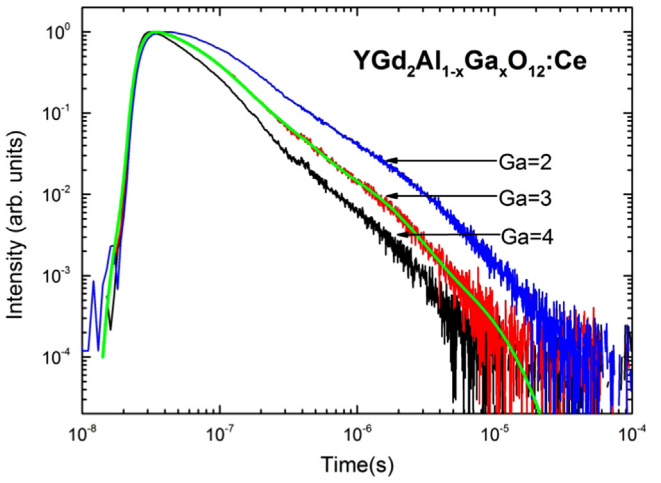


**Fig. 9.** Scintillation decays of the $YGd_2Al_{5-x}Ga_xO_{12}$:Ce ($x$=2,3,4) samples under excitation with ns-pulsed SXR. Solid line for $x$=3 is convolution of instrumental response (not in figure) and function $I(t)=1.2\times10^{-1}\exp(-t/49\ ns)+2.4\times10^{-2}\exp(-t/174\ ns)+3.6\times10^{-3}\exp(-t/945\ ns)+2.9\times10^{-4}\exp(-t/4420\ ns)$.

**Table 3**
Scintillation decay-time components and relative intensities of the $YGd_2Al_{5-x}Ga_xO_{12}$:Ce crystals.

| Crystal | Decay time (ns) [Relative intensity (%)] |
|---|---|
| $YGd_2Al_3Ga_2O_{12}$:Ce | 92 [37%], 431[22.2%], 1840 [27.6%], 8692 [13.2%] |
| $YGd_2Al_2Ga_3O_{12}$:Ce | 49 [40%],174 [28.4%], 945 [23.0%], 4420 [8.6%] |
| $YGd_2AlGa_4O_{12}$:Ce | 8 [6.4%], 51 [59.7%], 263 [19.4%], 1432 [14.5%] |

where $m_i$ are parameters obtained by a fit [42]. Afterwards, the relative fraction of the fast response part $K_{f/e}$ ($t$=0.5 μs) in the entire LY value ($t=\infty$) is obtained as

$$K_{f/e} = 1 - m_2/m_1. \quad (6)$$

The ratio of LY(0.5 μs) to LY(12 μs) and $K_{f/e}$ value for studied samples are collected in Table 2. A remarkable increase of the fast response part ($K_{f/e}$) is in the same trend with that of the fast component content in the scintillation response of $YGd_2Al_{5-x}Ga_xO_{12}$:Ce with increasing $Ga^{3+}$ content.

### 3.4. Scintillation decay under nanosecond pulsed SXR excitation

In Fig. 9 there are scintillation decays in enhanced time and dynamical scales under excitation by ns-pulsed SXR photons with energy within 300–400 eV [24]. With increasing gallium concentration the slower components of the decay are clearly diminished, the dominant scintillation decay time gets close to the PL one (see Fig. 6) and relative intensity of this component approaches 60%, see Table 3, which points to fast and efficient energy transfer from the host to $Ce^{3+}$ centers. The scintillation decays were approximated by four-exponential functions

$$I(t) = \sum_{i=1}^{4} A_i \exp[-t/t_i], \quad (7)$$

the parameters $A_i$ and $\tau_i$ stand for the pre-exponential factor and decay time, respectively, in the $i$-th decay component. The scintillation decay components and their relative intensities determined from a fit according to Eq. (7), from Fig. 9, are listed in Table 3. It is worth noting that similarly as in [33] for Ga=2 the

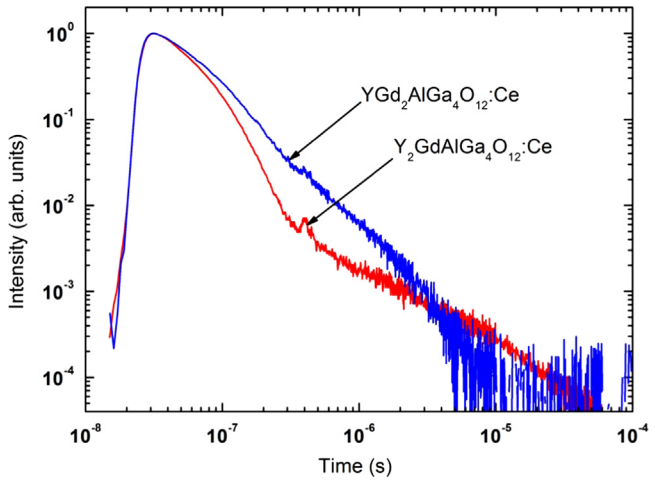


**Fig. 10.** Comparison of scintillation decays of $Y_2GdAlGa_4O_{12}$:Ce and $YGd_2AlGa_4O_{12}$:Ce samples.

dominant decay component shows the decay time almost 60% longer compared to PL one in Fig. 6 and the decay curve shows a sign of rising part which both point to degrading influence of slower energy transfer from the host to $Ce^{3+}$ centers.

In Fig. 10 a comparison of decay curves for $YGd_2AlGa_4O_{12}$:Ce and $Y_2GdAlGa_4O_{12}$:Ce [33] samples is provided. Higher concentration of Gd shows beneficial influence both on the temperature stability of $Ce^{3+}$ center and on the slowest decay component which becomes accelerated for any gallium concentrations.

## 4. Conclusions

In this work, the optical and scintillation characteristics of the $Ce^{3+}$- doped $YGd_2Al_{5-x}Ga_xO_{12}$ ($x$=2,3,4) single crystals are investigated. With increasing Ga content in the garnet host, the $5d_1$ absorption and emission bands shift toward higher energy due to the decrease in the crystal field splitting of the 5d levels. Thermal quenching of $5d_1$ excited state of $Ce^{3+}$ appears as dominant process in shaping temperature dependence of emission intensity and nanosecond decay times above 400 K. Thermally induced excited state ionization of $Ce^{3+}$ center is of minor importance and is evidenced above 300 K only in slow tails of nanosecond decays and by more sensitive delayed recombination decay technique. On the other hand, an acting subgap process of unclear origin was proposed to explain temperature dependence of the delayed radiative recombination decay the integral of which is increasing towards the lowest temperatures: A semiquantitative comparison of temperature dependence of delayed recombination intensity due to thermal ionization with that of actually observed has been performed. This experimental result needs further investigation.

High LY value of 38,000 ph/MeV obtained for the $YGd_2Al_2Ga_3O_{12}$:Ce sample is ~37% higher than that of a typical $Y_3Al_5O_{12}$:Ce Czochralski grown single crystal. The relative content of the fastest component in the scintillation response, related to the prompt radiative electron–hole recombination at $Ce^{3+}$ centers, increases with the Ga content. Small LY value decrease for the $YGd_2AlGa_4O_{12}$:Ce sample with the highest Ga content could be attributed to increasing thermal ionization of $5d_1$ excited state of the $Ce^{3+}$ emission center. Beneficial effect of increased Gd concentration in this sample set compared to earlier reported $Y_2GdAl_{5-x}Ga_xO_{12}$:Ce one [33] is demonstrated in the increased stability of $Ce^{3+}$ center against excited state ionization at the highest Ga concentration. Furthermore, the slowest decay part becomes accelerated for any Ga concentration.

## Acknowledgments

This work is supported by (i) the NRU Project of Thailand's Office of the Higher Education Commission, (ii) the JSPS Grant-in-Aid for Exploratory Research (AY), (iii) the funding program for next generation world-leading researchers, JSPS, and (iv) Supporting industry program, Ministry of Economy, Trade and Industry (METI). Financial support of Czech Science Foundation P204/12/0805 and MEYSLH14266 projects and EC FP7 Marie Curie Initial Training Network LUMINET, Grant agreement no. 316906 are also gratefully acknowledged.

## References

[1] R. Autrata, P. Schauer, J. Kvapil, J. Kvapil, J. Phys. E: Sci. Instrum. 11 (1978) 707.
[2] M. Moszynski, T. Ludziewski, D. Wolski, W. Klamra, L.O. Norlin, Nucl. Instrum. Methods Phys. Res. A 345 (1994) 461.
[3] A. Lempicki, M.H. Randles, D. Wisniewski, M. Balcerzyk, C. Brecher, A. J. Wojtowitz, IEEE Trans. Nucl. Sci. 42 (1995) 280.
[4] M. Nikl, E. Mihokova, J.A. Mares, A. Vedda, M. Martini, K. Nejezchleb, K. Blazek, Phys. Status Solidi B 181 (2000) R10.
[5] M. Nikl, A. Vedda, M. Fasoli, I. Fontana, V.V. Laguta, E. Mihokova, J. Pejchal, J. Rosa, K. Nejezchleb, Phys. Rev. B 76 (2007) 195121.
[6] W. Chewpraditkul, L. Swiderski, M. Moszynski, T. Szczesniak, A. Syntfeld-Kazuch, C. Wanarak, P. Limsuwan, IEEE Trans. Nucl. Sci. 56 (2009) 3800.
[7] J.A. Mares, A. Beitlerova, M. Nikl, N. Solovieva, C. D'Ambrosio, K. Blazek, P. Maly, K. Nejezchleb, F. de Notaristefani, Radiat. Meas. 38 (2004) 353.
[8] C. Dujardin, C. Mancini, D. Amans, G. Ledoux, D. Abler, E. Auffray, P. Lecoq, D. Perrodin, A. Petrosyan, K.L. Ovanesyan, J. Appl. Phys. 108 (2010) 013510.
[9] P. Dorenbos, IEEE Trans. Nucl. Sci. 57 (2010) 1162.
[10] M. Nikl, J. Pejchal, E. Mihokova, J.A. Mares, H. Ogino, A. Yoshikawa, T. Fukuda, A. Vedda, C. D'Ambrosio, Appl. Phys. Lett. 88 (2006) 141916.
[11] M. Fasoli, A. Vedda, M. Nikl, C. Jiang, B.P. Uberuaga, D.A. Andersson, K. J. McClellan, C.R. Stanek, Phys. Rev. B 84 (2011) 081102.
[12] Yu Zorenko, Opt. Spectrosc. 88 (2000) 551.
[13] N.J. Cherepy, J.D. Kuntz, Z.M. Seeley, S.E. Fisher, O.B. Drury, B.W. Sturm, T. A. Hurst, R.D. Sanner, J.J. Roberts, S.A. Payne, Proc. SPIE 7805 (2010) 78050I.
[14] K. Kamada, T. Endo, K. Tsutsumi, T. Yanagida, Y. Fujimoto, A. Fukabori, A. Yoshikawa, J. Pejchal, M. Nikl, Cryst. Growth Des. 11 (2011) 4484.
[15] K. Kamada, T. Yanagida, J. Pejchal, M. Nikl, T. Endo, K. Tsutsumi, Y. Fujimoto, A. Fukabori, A. Yoshikawa, J. Phys. D: Appl. Phys. 44 (2011) 505104.
[16] P. Dorenbos, J. Lumin. 134 (2013) 310.
[17] J.M. Ogiegło, A. Katelnikovas, A. Zych, T. Jüstel, A. Meijerink, C.R. Ronda, J. Phys. Chem. A 117 (2013) 2479.
[18] J. Ueda, K. Aishima, S. Tanabe, Opt. Mater. 35 (2013) 1952.
[19] Y. Wu, G. Ren, Opt. Mater. 35 (2013) 2146.
[20] M. Nikl, A. Yoshikawa, K. Kamada, K. Nejezchleb, C.R. Stanek, J.A. Mares, K. Blazek, Progr Cryst., Growth Charact. Mater. 59 (2013) 47.
[21] M. Moszynski, M. Kapusta, M. Mayhugh, D. Wolski, S.O. Flyckt, IEEE Trans. Nucl. Sci. 44 (1997) 1052.
[22] M. Bertolaccini, S. Cova, C. Bussolatti, in: Proceeding of the Nuclear Electronics Symposium, Versailles, France, 1968.
[23] J. Pejchal, M. Nikl, E. Mihóková, J.A. Mareš, A. Yoshikawa, H. Ogino, K. M. Schillemat, A. Krasnikov, A. Vedda, K. Nejezchleb, V. Múčka, J. Phys. D: Appl. Phys. 42 (2009) 055117.
[24] P. Bruza, V. Fidler, M. Nikl, J. Instrum. 6 (2011) P09007.
[25] C. Peth, XUV-Laserplasmaquellen fur die Absorptions-Spektroskopie und zeitaufgeloste Rontgenbeugung, Sierke-Verlag, Germany, 2009, ISBN 978-3-86844-101-7.
[26] M. Kucera, M. Nikl, M. Hanus, Z. Onderisinova, Phys. Status Solidi RRL 7 (2013) 571.
[27] V. Babin, M. Nikl, K. Kamada, A. Beitlerova, A. Yoshikawa, J. Phys. D: Appl. Phys. 46 (2013) 365303.
[28] Y. Pan, M. Wu, Q. Su, J. Phys. Chem. Solids 65 (2004) 845.
[29] W.W. Holloway, M.J. Kestigian, Opt. Soc. Am. 59 (1969) 60.
[30] J.M. Robertson, M.W. van Tol, W.H. Smits, J.P.H. Heynen, Philips J. Res. 36 (1981).
[31] A.B. Muñoz-García, L. Seijo, Phys. Rev. B 82 (2010) 184118.
[32] D.J. Robbins, J. Electrochem. Soc. 126 (1979) 1550.
[33] W. Chewpraditkul, D. Pánek, P. Brůža, W. Chewpraditkul, C. Wanarak, N. Pattanaboonmee, V. Babin, K. Bartosiewicz, K. Kamada, A. Yoshikawa, M. Nikl, J. Appl. Phys. 116 (2014) 083505.
[34] V.M. Bachmann, Studies on Luminescence and Quenching Mechanisms in Phosphors for Light Emitting Diodes, Ph.D. thesis, University of Utrecht, The Netherlands, 2007, ISBN:978-90-3934600-6.

[35] Y.N. Xu, W.Y. Ching, B.K. Brickeen, Phys. Rev. B 61 (2000) 1817.
[36] M. Fasoli, A. Vedda, E. Mihokova, M. Nikl, Phys. Rev. B 85 (2012) 085127.
[ 37] E. Mihóková, K. Vávrů, K. Kamada, V. Babin, A. Yoshikawa, M. Nikl, Radiat. Meas. 56 (2013) 98.
[38] K. Brylew, W. Drozdowski, A.J. Wojtowicz, K. Kamada, A. Yoshikawa, J. Lumin. 154 (2014) 452.
[39] A. Gektin, A. Belsky, A. Vasil'ev, IEEE Trans. Nucl. Sci. 61 (2014) 262.
[40] V. Babin, V. Gorbenko, A. Krasnikov, A. Makhov, E. Mihokova, M. Nikl, S. Zazubovich, Yu Zorenko, Phys. Status Solidi B 249 (2012) 1039.
[41] W. Chewpraditkul, N. Pattanaboonmee, W. Chewpraditkul, K. Kamada, A. Yoshikawa, M. Nikl, Appl. Mech. Mater. 709 (2015) 390.
[42] P. Prusa, M. Nikl, J.A. Mares, M. Kucera, K. Nitsch, A. Beitlerova, Phys. Status Solidi A 206 (2009) 1494.